Water Science & Technology: Water Supply

Granulation of Fe-Al-Ce nano-adsorbent for fluoride removal from drinking water using inorganic binder

Chao-Li Su, Lin Chen, Ting-Jie Wang, Li-Xin Yu and Yong Jin

ABSTRACT

Nano-adsorbents usually have high fluoride adsorption capacity. However, they cannot be used in packed beds because of their low hydraulic conductivity. Granulation with organic binder usually causes a great loss of adsorption capacity due to the active sites of the adsorbent being extensively occupied by the organic binder. Using inorganic sol as a binder is expected to have a potential for reducing the loss of adsorption capacity. In this paper, aluminium, zirconium, titanium and silica sol were employed as binders for Fe-Al-Ce nano-adsorbent granulation. The nano-adsorbent was mixed with sol and dried to form lumps, then calcinated and ground into powder. The morphology, adsorption capacity and structure of the compound powder were analysed. As an optimization, aluminium sol was selected as a binder in the granulation of Fe-Al-Ce nano-adsorbent using extrusion method. The effects of sol on the adsorbent and the granule structure were characterized. The granules showed a high adsorption capacity, reaching over 90% capacity of Fe-Al-Ce nano-adsorbent, much higher than that of using acrylic-styrene copolymer latex as a binder in our previous research. It is inferred that aluminium sol is a suitable binder which does no damage to the active hydroxyl group of Fe-Al-Ce adsorbent.

Key words | adsorbent, adsorption capacity, drinking water, granulation, inorganic binder

Chao-Li Su
Lin Chen
Ting-Jie Wang (corresponding author)
Li-Xin Yu
Yong Jin
Department of Chemical Engineering,
Tsinghua University,
Beijing 100084,
China
E-mail: wangtj@tsinghua.edu.cn

INTRODUCTION

Fluoride present in drinking water is essential for human health. However, excessive fluoride ion existing in drinking water is harmful to health and causes dental and skeletal fluorosis (Ayoob & Gupta 2006). More than 200 million people worldwide rely on drinking water with fluoride concentration that exceeds the WHO guideline of 1.5 mg/L (Bhatnagar *et al.* 2011). Adsorption has been the most widely used technology for fluoride removal from drinking water for its low cost, high effectiveness and easy operation (Meenakshi & Maheshwari 2006).

Recent research on adsorbents for fluoride removal in drinking water has focused on nano-adsorbents. Nano-adsorbents usually have high fluoride adsorption capacity due to their large specific surface area and high activity (Kumar *et al.* 2011; Mohapatra *et al.* 2012). However, they cannot be used in packed beds because of their low hydraulic conductivity and they need to be granulated at a large

size of about 1–2 or 2–3 mm. Researchers have developed some techniques of coating nano-adsorbent onto sand such as iron oxide-coated sand (Lai *et al.* 2000). Polymers were introduced to immobilize aluminosilicate clays on a silica support to improve the coating amount (Jerez *et al.* 2006).

An Fe-Al-Ce trimetal oxide nano-adsorbent (Fe-Al-Ce) has emerged in recent studies due to its high fluoride adsorption capacity (Wu *et al.* 2007). In our previous research, the Fe-Al-Ce was spray-coated onto sand or glass bead using an acrylic-styrene copolymer latex as a binder in a fluidized bed. The adsorbent granules showed a high mechanical strength and some loss of adsorption capacity (Chen *et al.* 2011). The active sites on the Fe-Al-Ce surface were partly lost due to a chemical bond formation between the polymer and Fe-Al-Ce (Dou 2006; Chen *et al.* 2009). This paper aims to reduce the loss of

adsorption capacity by replacing the organic binder with inorganic sol.

MATERIAL AND METHODS

Material

$FeSO_4 \cdot 7H_2O$, $Al_2(SO_4)_3 \cdot 12H_2O$ and $Ce(SO_4)_2 \cdot 4H_2O$ used were of analytical grade (Chemical Engineering Company of Beijing, China). The other chemicals used were of analytical reagent (AR) grade.

Adsorbent and sol binder preparation

$FeSO_4 \cdot 7H_2O$, $Al_2(SO_4)_3 \cdot 12H_2O$ and $Ce(SO_4)_2 \cdot 4H_2O$ were dissolved in deionized water to form a mixed solution with concentrations of 0.1, 0.2 and 0.1 M, respectively. A 6 M NaOH solution was slowly titrated into the mixed solution until the pH reached 9.5. The precipitate obtained was vacuum filtrated and washed with deionized water. The product was Fe-Al-Ce trimetal hydroxide adsorbent, which has a high specific surface area of 90 m^2/g and diameter of 40 nm. The morphology of Fe-Al-Ce is shown in Figure 1. The Fe-Al-Ce was kept in deionized water.

Aluminium sol was prepared by sol-gel method using aluminium isopropoxide as precursor (Buelna & Lin 1999). Aluminium isopropoxide was dissolved in deionized water and hydrolysed at 85 °C. After hydrolysis, 2% HNO_3
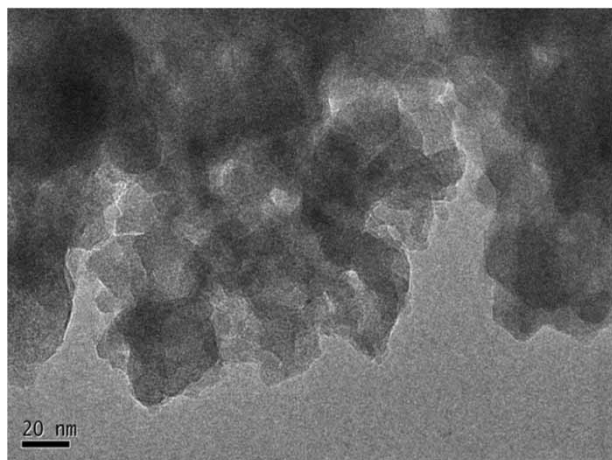

Figure 1 | Morphology of Fe-Al-Ce adsorbent.

solution was slowly titrated into the solution until a transparent sol was obtained. Then, the aluminium sol was aged at 90 °C for 3 h.

Zirconium sol was prepared by the sol-gel method using zirconium oxychloride as precursor (Li 2003). Zirconium oxychloride was dissolved in ethanol solution, of which the volume fraction of ethanol to deionized water was 0.5, to form a solution with concentration of 1 M. Zirconium oxychloride was hydrolysed in the presence of hydrogen peroxide with continual stirring. Then an ammonia solution of 1.5 M was slowly titrated into the solution until the pH reached 5. After titration the solution was heated to 90 °C in a thermostatic water bath, and the produced ammonia and hydrogen chloride gas due to heating were evacuated.

Titanium sol was prepared by sol-gel method using tetrabutyl orthotitanate as precursor (Fu *et al.* 2009). Tetrabutyl orthotitanate was hydrolysed in ethanol solution. Glacial acetic acid was added to the solution to control the hydrolysis rate. The solution pH 2 was maintained by adjusting with hydrochloric acid, then the solution was aged at 90 °C for 3 h.

Silica sol used was a commercial product from Qingdao Haiyang Chemical Co., Ltd.

Sampling and characterization

Compound powder

The Fe-Al-Ce was mixed with different sol to form slurry with the mass ratio adsorbent/sol of 1/0.5. The slurry was dried in an oven at 80 °C. After drying, the slurry of Fe-Al-Ce and sol formed lumps. Part of the lumps was calcinated at 350 °C for 1.5 h. The uncalcinated and calcinated lumps were ground into powder for further characterization.

Granulation

The Fe-Al-Ce was granulated using extrusion method with aluminium sol. The Fe-Al-Ce was mixed with aluminium sol and diluted with deionized water to form slurry with a mass ratio adsorbent/sol of 1/0.5. After stirring, the slurry was dried in an oven until it became a mixed mud. The mixed mud was squeezed through a mould under a pressure

of 20 N. After drying, the granules were calcinated at 500 °C for 3 h. The mould is shown in Figure 2.

Characterization

Transmission electron microscopy (JEM-2011, JEOL Co., Japan), scanning electron microscopy (JSM 7401, JEOL Co., Japan), Fourier transform infrared (FTIR) spectroscopy (Nicolet 5700, Thermo Nicolet, Madison, WI, USA) and thermogravimetric analysis (TGA/DSC1/16600HT, Mettler-Toledo, Germany) were used to examine the morphology and structure of the sol, nano-adsorbent, compound powder and granules. The fluoride ion concentration of the solution was measured with a fluoride selective electrode connected to an ion meter (PXS-450, Shanghai Kang-Yi Instruments Co., Ltd, China).

Fluoride adsorption capacity determination

Fluoride containing solutions were prepared by dissolving NaF into deionized water. A 50 mg/L fluoride solution was prepared by dissolving 0.2210 g NaF in 2,000 mL of deionized water. The above solution was diluted to prepare a 10 mg/L fluoride solution. The fluoride adsorption capacity of different samples was determined by adding a known mass of sample to 100 mL of the fluoride containing solution. Doses of different samples for sol, Fe-Al-Ce, compound powder, and granulated adsorbents were 1, 1, 1.5 and 1.5 g/L, respectively. The test solution was shaken at 180 rpm and kept at 25 °C for 24 h during the adsorption. After adsorption, the adsorbent was filtered and the filtrate was analysed. The
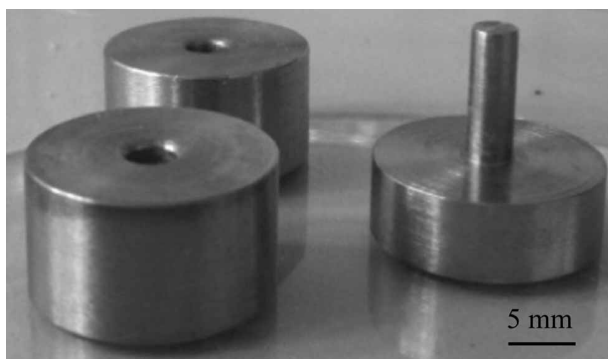

5 mm

Figure 2 | Image of the granulation mould.

adsorption capacity was calculated using:

$$q_e(\text{mg/g}) = \frac{C_0 - C_f}{m} \times V \tag{1}$$

$$q_e(\text{mg/g Fe-Al-Ce}) = \frac{C_0 - C_f}{m \times R} \times V \tag{2}$$

where C_0 is the initial fluoride concentration, mg/L; C_f is the final fluoride concentration after adsorption, mg/L; V is the volume of the solution containing fluoride ions, L; m is the adsorbent mass, g; R is the mass fraction of Fe-Al-Ce in compound powder or granulated adsorbent, i.e. for adsorbent/sol of 1/0.5, the fraction is 2/3 in this text.

RESULTS AND DISCUSSION

Inorganic sol binder

Figure 3 shows the morphology of different sols. Aluminium sol was roughly flaky with a size of about 20 nm. Zirconium sol was roughly spherical with a size of about 15 nm and aggregated in chains. Titanium sol is very small in size and easily aggregated. Silica sol was spherical with a size of about 40 nm and is aggregated in chains.

As shown in Figure 4, compound powder using aluminium, zirconium or silica sol as a binder has a rough surface. There are many Fe-Al-Ce nano particles on the surface of these three compound powders. However, compound powder using titanium sol as a binder has a smooth surface and a dense structure. It is supposed that titanium sol reacted with Fe-Al-Ce in the drying process and produced new material.

Fluoride adsorption capacity of compound powder

In order to compare the inorganic sol properties, the fluoride adsorption capacity of sol and compound powder with different sol was measured. Because the heat treatment usually affects the adsorbent properties significantly, the adsorption capacities before and after calcination were also measured. Table 1 shows the fluoride adsorption capacities of sol, Fe-Al-Ce and compound powder.
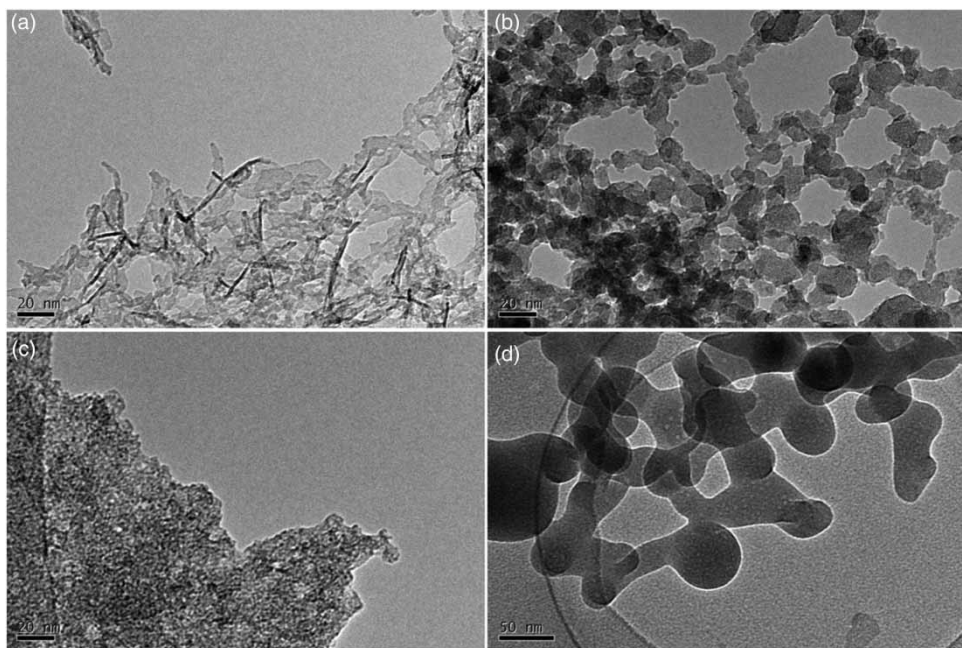
Figure 3 | Morphology of inorganic sol. (a) Aluminium sol; (b) zirconium sol; (c) titanium sol; (d) silica sol.
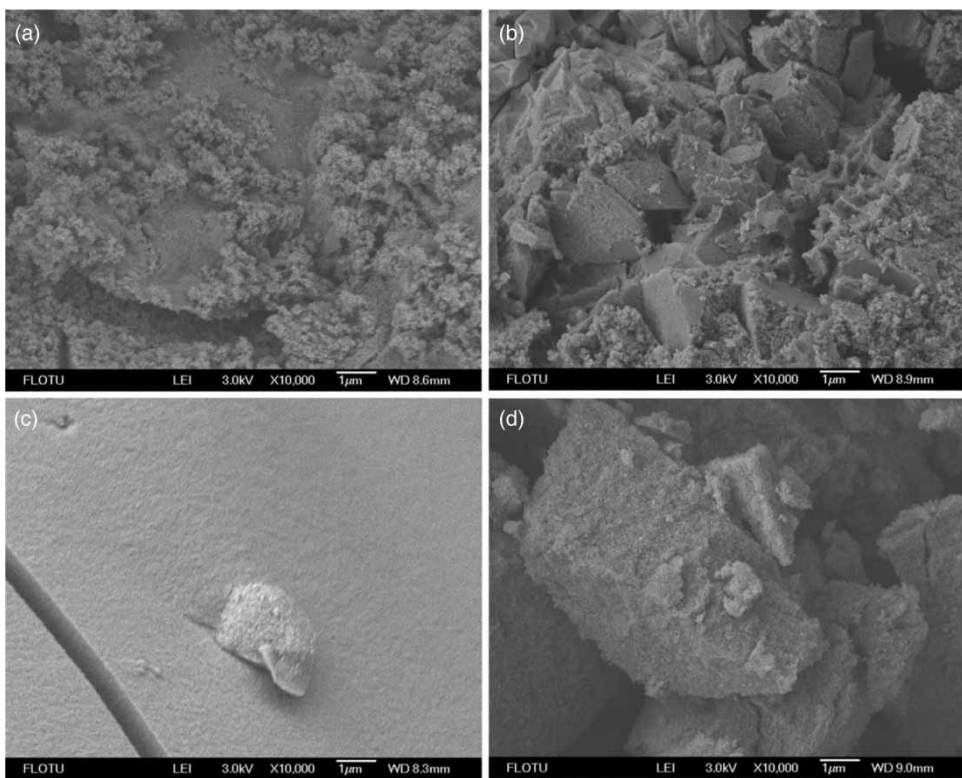
Figure 4 | Surface morphology of compound powder with different sols. (a) Aluminium sol; (b) zirconium sol; (c) titanium sol; (d) silica sol.

Table 1 | Fluoride adsorption capacity of sol, Fe-Al-Ce and compound powder[a]

		Al	Zr	Ti	Si
q_e of sol (mg/g)		29.81	47.99	26.12	2.04
q_e of compound powder (mg/g Fe-Al-Ce)	Uncalcinated	45.63	39.48	12.75	47.57
	Calcinated (350 °C)	45.86	36.86	40.58	48.06
q_e of Fe-Al-Ce (mg/g)	Uncalcinated	47.55			
	Calcinated (350 °C)	46.67			

[a]The initial fluoride concentration is 50 mg/L; dose for sol, Fe-Al-Ce, compound powder was 1, 1 and 1.5 g/L, respectively.

It can be seen from Table 1 that aluminium, zirconium and titanium sol all have a relatively high adsorption capacity themselves, while silica sol has not. After compounding with Fe-Al-Ce, the compound powder using aluminium or silica sol as a binder has nearly the same adsorption capacity as Fe-Al-Ce. This indicates that aluminium or silica sol does not reduce the adsorption capacity of Fe-Al-Ce when it is used as a binder. Although zirconium sol has a high adsorption capacity itself, the adsorption capacity of compound powder was lower than both Fe-Al-Ce and zirconium sol. This indicates that zirconium sol caused a certain loss to the adsorption capacity of Fe-Al-Ce. Compound powder using titanium sol as a binder has the lowest adsorption capacity. As discussed regarding the surface morphology, it is inferred that titanium sol reacted with Fe-Al-Ce adsorbent and damaged the active sites, causing the great loss of adsorption capacity.

Table 1 shows that the adsorption capacity of Fe-Al-Ce did not change much after calcination. The adsorption capacity of compound powder using titanium sol as a binder has a significant increase after calcination. This confirms further that the adsorption capacity was not from the Fe-Al-Ce adsorbent but from new material produced during the compounding process, because the adsorption capacity of Fe-Al-Ce did not increase after calcination. The adsorption capacity of compound powder using aluminium or silica sol as a binder did not change much either. Therefore, calcination can be designed in the granulation experiment when using aluminium or silica sol as a binder and it does not reduce the adsorption capacity.

Calcination of compound powder

Figure 5 shows the thermogravimetry curve of compound powder of different sols. From Figure 5, some structure information of compound powder can be analysed. For titanium sol, the compound powder has more weight loss than either titanium sol or Fe-Al-Ce adsorbent, which is against the mixing rule. The weight loss plateau of titanium sol at 450–900 °C or Fe-Al-Ce adsorbent at 300–650 °C disappeared in the curve of compound powder, as shown in Figure 5(c). This confirms that titanium sol reacted with Fe-Al-Ce adsorbent, producing a new material. The introduction of titanium sol damaged the main structure of Fe-Al-Ce adsorbent and caused the low adsorption capacity of compound powder. The weight loss of the other three compound powders was between sol and Fe-Al-Ce. The curves of other three compound powders also have the weight loss plateau of Fe-Al-Ce, which indicates that the main structure of Fe-Al-Ce was not damaged during compounding using aluminium, zirconium or silica sol as a binder.

The promising inorganic binder should not damage the active site of Fe-Al-Ce and keeps a high adsorption capacity after compounding with Fe-Al-Ce. From the above analysis, it is concluded that aluminium and silica sols do not damage the main structure of Fe-Al-Ce or reduce the adsorption capacity, and they are both promising binders.

Table 1 shows that the adsorption capacity of Fe-Al-Ce changed little before and after calcination at 350 °C. In the thermogravimetry curve of Fe-Al-Ce, the first weight loss peak finished at about 300 °C and then the curve entered the plateau until 650 °C, see Figure 5(c). This indicates that the first weight loss does not affect the adsorption capacity of Fe-Al-Ce. So calcination at temperatures below 650 °C should not reduce the adsorption capacity. Therefore, a calcination temperature of 500 °C and calcination time of 3 h were set in the heat treatment of granules of compound powder.

Granulation of compound powder

The compound powder was granulated by extrusion moulding using aluminium sol as a binder. The surface
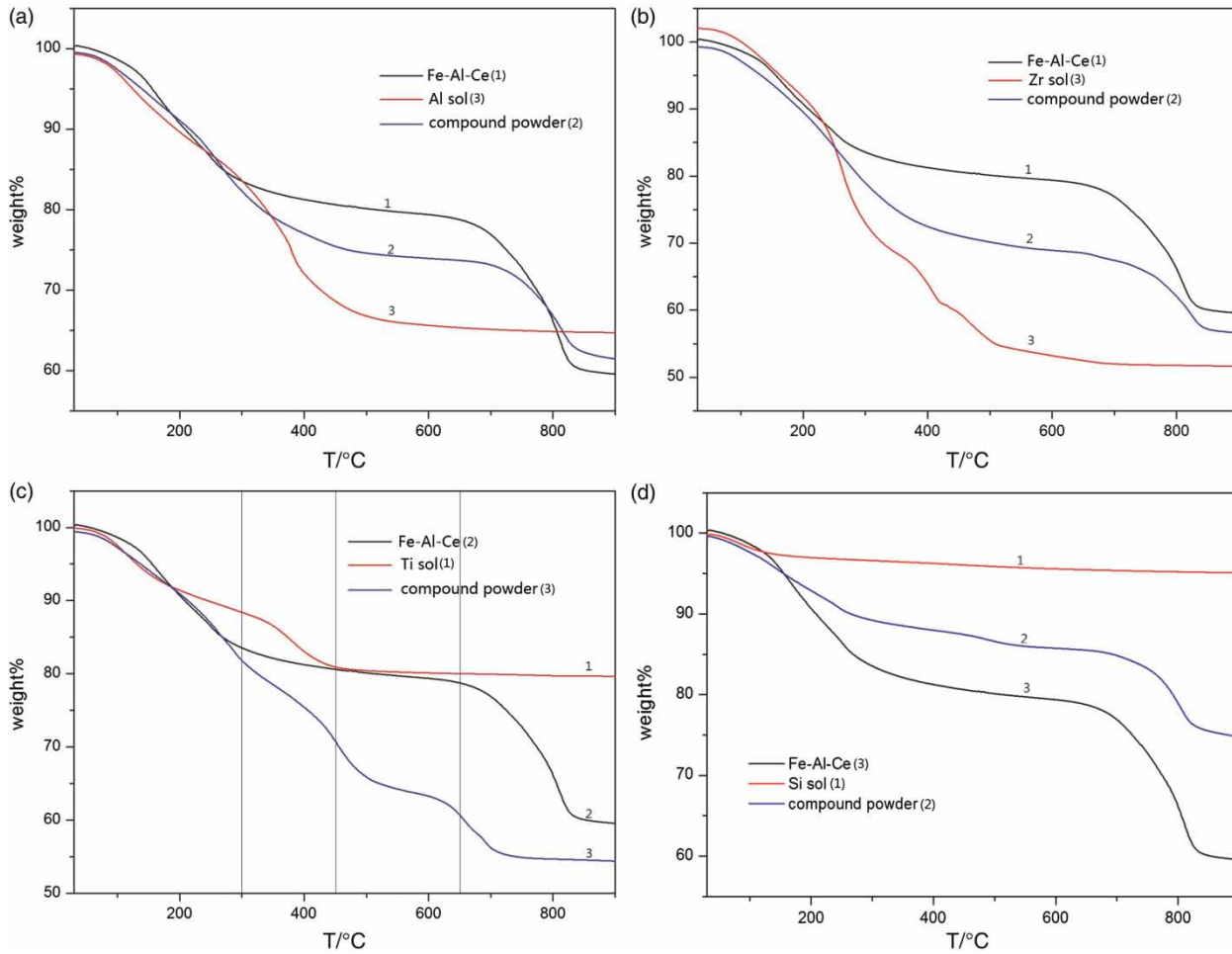
Figure 5 | Thermogravimetry of compound powder of different sol.

morphology of the granulated adsorbents is shown in Figure 6. The cylinder granule has a diameter of about 2.5 mm and a length of 2–4 mm. Figure 6 shows that Fe-Al-Ce was bound by aluminium sol and has a rough surface.

The fluoride adsorption capacity of the granulated adsorbent is shown in Table 2.

In the fluoride adsorption capacity determination of granulated adsorbents, the initial fluoride concentration
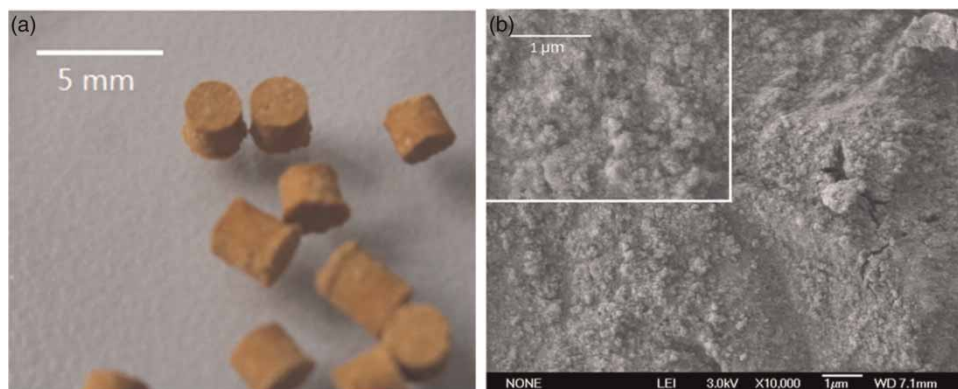
Figure 6 | Morphology of the granulated adsorbents by extrusion moulding using aluminium sol as a binder. (a) Granules; (b) surface morphology.

Table 2 | Fluoride adsorption capacity of the granulated adsorbent[a]

Fluoride adsorption capacity	Uncalcinated granules	Calcinated granules (500 °C)	Fe-Al-Ce
(mg/g Fe-Al-Ce)	7.78	9.04	9.63

[a]The initial fluoride concentration is 10 mg/L; dose of the granules and Fe-Al-Ce is 1.5 and 1 g/L, respectively.

was reduced to 10 mg/L. This concentration was close to that of underground water containing fluoride. As shown in Table 2, the granulated adsorbent after calcination has a high adsorption capacity, which reached more than 90% of Fe-Al-Ce. The residual fluoride concentration was below 1 mg/L. This shows that calcination at 500 °C for 3 h increased the adsorption capacity compared with the uncalcinated granules. It is supposed that the calcination at 500 °C caused pore formation inside the granule so that more Fe-Al-Ce was exposed. Meanwhile, the active site of Fe-Al-Ce was not damaged at 500 °C so the adsorption capacity of granulated adsorbents increased.

The active site for fluoride adsorption is from the hydroxyl group on the Fe-Al-Ce surface (Dou 2006). The FTIR spectra of aluminium sol, Fe-Al-Ce, granule before and after adsorption are shown in Figure 7. The absorbance peak of bending vibrations of the hydroxyl group (near $1,125 \text{ cm}^{-1}$) was considered the characteristic peak of active hydroxyl group for fluoride adsorption (Zhang *et al.* 2005; Chen *et al.* 2009). As shown in Figure 7, the characteristic peak of active hydroxyl group decreased significantly
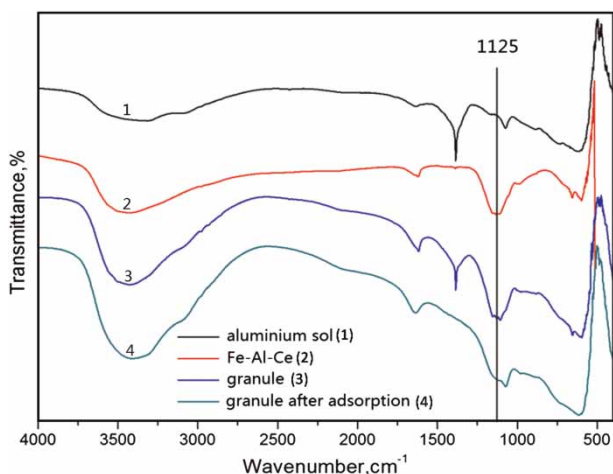
Figure 7 | FTIR spectra of granulated adsorbent using aluminium sol as a binder.

after adsorption of fluoride. This indicated that the active hydroxyl group on the Fe-Al-Ce surface had reacted with the fluoride ions in the adsorption process, and the characteristic peak of active hydroxyl group did not decrease after granulation using aluminium sol as a binder. It showed that aluminium sol did not damage the active hydroxyl group or reduce the adsorption capacity. The FTIR spectra proved that using aluminium sol as a binder does not cause much loss of adsorption capacity of Fe-Al-Ce adsorbent.

CONCLUSIONS

Aluminium, zirconium, titanium and silica sol were employed as a binder for Fe-Al-Ce granulation. The interaction between sol and Fe-Al-Ce was analysed. Titanium sol can react with Fe-Al-Ce during compounding and make the adsorption capacity decrease significantly. Zirconium sol causes a certain loss to the adsorption capacity of compound powder compared with itself and Fe-Al-Ce. Aluminium or silica sol do not damage the active site of Fe-Al-Ce, and the compound powder using aluminium or silica sol as a binder has an adsorption capacity as high as that of Fe-Al-Ce.

Granulated adsorbents were prepared by extrusion moulding using aluminium sol as a binder. The adsorption capacity of granulated adsorbents was relatively high and even higher after calcination at 500 °C, reaching over 90% adsorption capacity of Fe-Al-Ce. Aluminium sol causes no damage to the active hydroxyl group of Fe-Al-Ce adsorbent. Granulation adsorbents using aluminium sol as a binder have an adsorption capacity much higher than using acrylic-styrene copolymer latex as a binder in our previous research (Chen *et al.* 2011).

ACKNOWLEDGEMENTS

REFERENCES

Ayoob, S. & Gupta, A. K. 2006 Fluoride in drinking water: a review on the status and stress effects. *Crit. Rev. Environ. Sci. Technol.* **36** (6), 433–487.

Bhatnagar, A., Kumar, E. & Sillanpää, M. 2011 Fluoride removal from water by adsorption – a review. *Chem. Eng. J.* **171** (3), 811–840.

Buelna, G. & Lin, Y. S. 1999 Sol-gel-derived mesoporous gamma-alumina granules. *Micropor. Mesopor. Mater.* **30** (2–3), 359–369.

Chen, L., Wu, H. X., Wang, T. J., Jin, Y., Zhang, Y. & Dou, X. M. 2009 Granulation of Fe-Al-Ce nano-adsorbent for fluoride removal from drinking water by spray coating on sand in a fluidized bed. *Powder Technol.* **193** (1), 59–64.

Chen, L., Wu, H. X., Wang, T. J., Jin, Y., Zhang, Y. & Dou, X. M. 2011 Optimization of a Fe-Al-Ce nano-adsorbent granulation process that used spray coating in a fluidized bed for fluoride removal from drinking water. *Powder Technol.* **206** (3), 291–296.

Dou, X. M. 2006 Adsorption Mechanism and Application Study of Fe-Ce Oxide Adsorbent for Arsenic Removal. Doctoral Dissertation, Chinese Academy of Science.

Fu, Y., Jin, Z. G., Ni, Y., Du, H. Y. & Wang, T. 2009 Microstructure, optical and optoelectrical properties of mesoporous nc-TiO$_2$ films by hydrolysis-limited sol-gel process with different inhibitors. *Thin Solid Films* **517** (19), 5634–5640.

Jerez, J., Flury, M., Shang, J. Y. & Deng, Y. J. 2006 Coating of silica sand with aluminosilicate clay. *J. Colloid Interface Sci.* **294** (1), 155–164.

Kumar, E., Bhatnagar, A., Kumar, U. & Sillanpää, M. 2011 Defluoridation from aqueous solutions by nano-alumina: characterization and sorption studies. *J. Hazard. Mater.* **186** (2–3), 1042–1049.

Lai, C. H., Lo, S. L. & Chiang, H. L. 2000 Adsorption/desorption properties of copper ions on the surface of iron-coated glass bead using BET and EDAX analyses. *Chemosphere* **41** (8), 1249–1255.

Li, M. 2003 Making spherical zirconia particles from inorganic zirconium aqueous sols. *Powder Technol.* **137** (1–2), 95–98.

Meenakshi, S. & Maheshwari, R. C. 2006 Fluoride in drinking water and its removal. *J. Hazard. Mater.* **137** (1), 456–463.

Mohapatra, M., Hariprasad, D., Mohapatra, L., Anand, S. & Mishra, B. K. 2012 Mg-doped nano ferrihydrite – a new adsorbent for fluoride removal from aqueous solutions. *Appl. Surf. Sci.* **258** (10), 4228–4236.

Wu, X. M., Zhang, Y., Dou, X. M. & Yang, M. 2007 Fluoride removal performance of a novel Fe-Al-Ce trimetal oxide adsorbent. *Chemosphere* **69** (11), 1758–1764.

Zhang, Y., Yang, M., Dou, X. M., He, H. & Wang, D. S. 2005 Arsenate adsorption on an Fe-Ce bimetal oxide adsorbent: role of surface properties. *Environ. Sci. Technol.* **39** (18), 7246–7253.